Online Balance Controllers for a Hopping and Running Humanoid Robot

Baek-Kyu Cho [a,b], **Jung-Hoon Kim** [c,*] **and Jun-Ho Oh** [d]

[a] *Department of Brain Robot Interface, the Computational Neuroscience Laboratories, Advanced Telecommunications Research Institute International (ATR), Kyoto 619-0288, Japan,*

[b] *National Institute of Information and Communications Technology (NiCT), Kyoto 619-0288, Japan, and swan0421@gmail.com*

[c] *Construction Robot and Automation Laboratory, Department of Civil and Environmental Engineering, Yonsei University 134, Shinchon-dong, Seodaemun-gu, Seoul, 120-749, South Korea and junghoon@yonsei.ac.kr*

[d] *Hubo-Lab, Department of Mechanical Engineering, KAIST, 335, Gwahangno, Yeseong-gu, Daejeon, 307-701, South Korea, and jhoh@kaist.ac.kr*

Abstract

This paper describes online balance controllers for running in a humanoid robot and verifies the validity of the proposed controllers via experiments. To realize running in the humanoid robot, the overall control structure is composed of an offline controller and an online controller. The main purpose of the online controller is to maintain dynamic stability while the humanoid robot hops or runs. The online controller is composed of the posture balance control in the sagittal plane, the transient balance control in the frontal plane, and the swing ankle pitch compensator in the sagittal plane. The posture balance controller makes the robot maintain balance using an IMU (inertial measurement unit) sensor in the sagittal plane. The transient balance controller makes the robot keep its balance in the frontal plane using gyros attached to each upper leg. The swing ankle pitch compensator prevents the swing foot from hitting the ground at unexpected times while the robot runs forward. HUBO2 was used for the running experiment. It was designed for the running experiment, and is lighter and more powerful than the previous walking robot platform, HUBO. With the proposed controllers, HUBO2 ran forward stably at a maximum speed of 3.24km/h and this result verified the effectiveness of the proposed algorithm. In addition, in order to show the contribution of the stability,

---

[*] To whom correspondence should be addressed. E-mail: junghoon@yonsei.ac.kr

the running performance according to existence of each controller was described by experiment.

Keywords

Humanoid, running, biped robot, HUBO2

1. Introduction

The appearance of new humanoid robot is not a surprise anymore. Various humanoid robots are announced every year through exhibitions, the internet, TV, and so on. One of the ultimate purposes of these robots is to help human beings. With intelligent abilities such as manipulation, mobility, navigation, recognition and human-robot interaction, humanoid robots will provide service to human beings in houses or companies, improving the quality of life. For example, the ASIMO of Honda has given many demonstrations of delivering beverages to people on a tray, helping elderly people, and so on [1]. In addition, HUBO [2] and HRP-2[3] have given similar demonstrations. HRP-2 has also given demonstrations of tele-operation of a remote excavator in the construction site and cooperation with humans in installing panels. However, if the safety of the robot is not perfectly guaranteed, the robot cannot help people but can cause harm to them. Therefore, a controller that guarantees stability can be regarded as the most important issue in the real application of robots to our daily lives.

Locomotion is classified into walking and running. Even though running is more unstable than walking, the fast mobility of running is very attractive. For this reason, the study of running is ongoing in many places. The pace setters of humanoid running are ASIMO of Honda [4][5] and Partner robot of Toyota [6]. According to an announcement in 2005, the newest version of ASIMO can walk at a maximum rate of 2.7km/h and can run at a maximum rate of 6km/h. In addition, the Partner robot can run at a maximum rate of 7km/h, which is faster than ASIMO. Besides, QRIO of Sony [7], HRP-2LR of AIST [8], and others are being used in further research into running. However, the running algorithms of the ASIMO and Partner robot have not been announced in public, and the other robots except for ASIMO and Partner robot do not show strong running ability. Also, Chevallereau et al. tried to realize running with the planar robot, but it ran only 6 steps [9]. Even though it is not a humanoid robot, Raibert realized running with 3D Biped [10].

Therefore, this paper describes an online controller to raise the stability when a humanoid robot hops

or runs. The validity of the controller is verified by experiment using HUBO2. This robot was developed at KAIST in 2008. Since it is lighter and more powerful than HUBO, it is suitable for use in research about running. The running pattern of HUBO2 is generated offline by the running pattern generation method, which has been studied in previous research [11]. The running pattern is generated with the Poincare map of the single step running and its fixed point to make natural and periodic running pattern. The fixed point is numerically calculated. In addition, an online controller for running is applied to HUBO2 in real time to realize stable running.

This paper is organized as follows: In Section 2, the humanoid robot used in this paper, HUBO2, is explained. In Section 3, the online controller for running in humanoid robots is explained. The online controller is composed of three controllers. First, the posture balance controller in the sagittal plane makes the humanoid robot maintain its balance and reduces the vibration in the sagittal plane. Second, the transient balance control in the frontal plane prevents the humanoid robot from falling in the frontal plane. Third, the swing ankle pitch compensator in the sagittal plane keeps the swing foot of the humanoid robot from touching the ground while the humanoid robot runs. In Section 4, the controllers are verified in experiments. Finally, the last section concludes the paper.

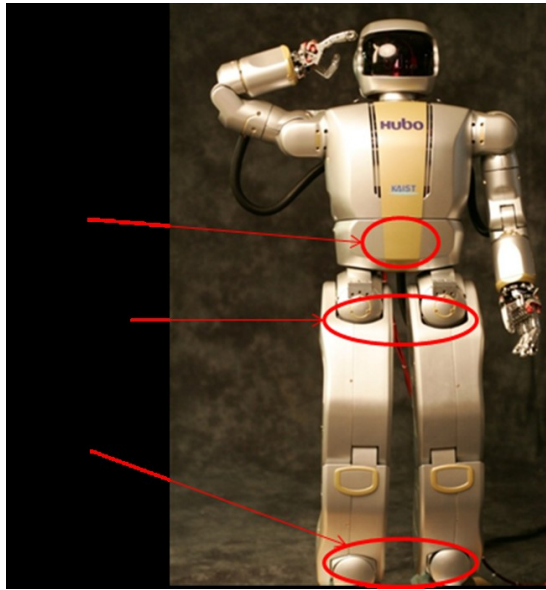## 2. Overview of the Humanoid Robot, HUBO2

Figure 1. HUBO2

HUBO2, developed in 2008, is shown in Fig. 1. It has a total of 40 DOFs (Degrees of Freedom) including 12 DOFs in the lower limbs, 1 DOF in the waist, 14 DOFs in the two arms, 10 DOFs in the two hands, and 3 DOFs in the neck. In the development of HUBO2, the design objective was focused on a reduction in weight and an increase in actuator power. Therefore, HUBO2 is more suitable than HUBO for running research. The total weight of HUBO2, including battery, exterior case, computer, sensors, controllers and amplifiers is 45 kg. This is only 69 percent of the weight of HUBO, which weighed 65 kg. To reduce the weight and produce the high power, the CSF type harmonic drive gear and 150W DC motor used in HUBO were replaced with an SHD type harmonic drive gear and 200W BLDC motor. Also, the synthetic resins are attached at the four corners of both soles to protect the robot from the landing impact.

Table 1. HUBO vs. HUBO2

	HUBO	HUBO2
Total weight	65 kg	45 kg
Weight of major motor	0.447 kg	0.283 kg

	(150W DC motor)	(200W BLDC motor)
Weight of major harmonic drive	0.947 kg	0.511 kg

Also, HUBO2 uses a distributed control system: the main computer managing the overall operation of the robot and the joint motor controllers (JMCs) controlling the motor of the robot are connected through CAN (Controller Area Network) communication. If the main computer sends position commands to JMC, each JMC control assigns motor to move to the commanded position. Some sensory devices attached on the robot are used for posture control and motion control, and these communicate with the main computer through the CAN. Since the main computer is attached inside the humanoid robot, wireless LAN is used to access the main computer.

In HUBO, the main computer and the JMCs communicate every 10 milliseconds by CAN. In order to realize running, 100Hz of control loop is not sufficient. Therefore, in HUBO2, the lower body of the robot and the sensory devices that mainly affect stability communicate every 5 milliseconds with the main computer, while the upper body and the head of robot communicate every 10 milliseconds with the main computer.

In this study, an inertia measurement unit (IMU), a gyro, and force/torque (F/T) sensors are used. An IMU sensor is attached to the upper body of the robot and measures the angles and angular velocities against the ground in the sagittal and frontal planes. The IMU sensor is composed of an inclinometer and a gyro. Other gyro sensors are used to measure the angular velocity of the stance leg in the frontal plane; these sensors are attached to both thighs, as shown in Fig. 1. Also, F/T sensors are attached at the ankle joints and measure the normal force in the vertical direction and two moments along the roll and pitch axes. They are used to detect the landing and flying timings.

3. Online Controllers for Running

To realize locomotion of a humanoid robot, an offline controller and an online controller are required. The offline controller calculates such things as walking or running patterns and the online controller works based in real-time on sensor feedback when the robot moves. The running pattern included in the offline controller was dealt with in the previous research [9] and the online controller, which makes a stable balance when the robot hops or runs, is described in this paper.

In Fig. 2, the control structure of HUBO2 used in this research is shown. The left part is the offline controller. According to the desired running velocity, all of joint trajectories are obtained by the offline controller, which is the running pattern generator. On the other hand, the right part is the online controller, which enables the humanoid robot to maintain balance in real-time.
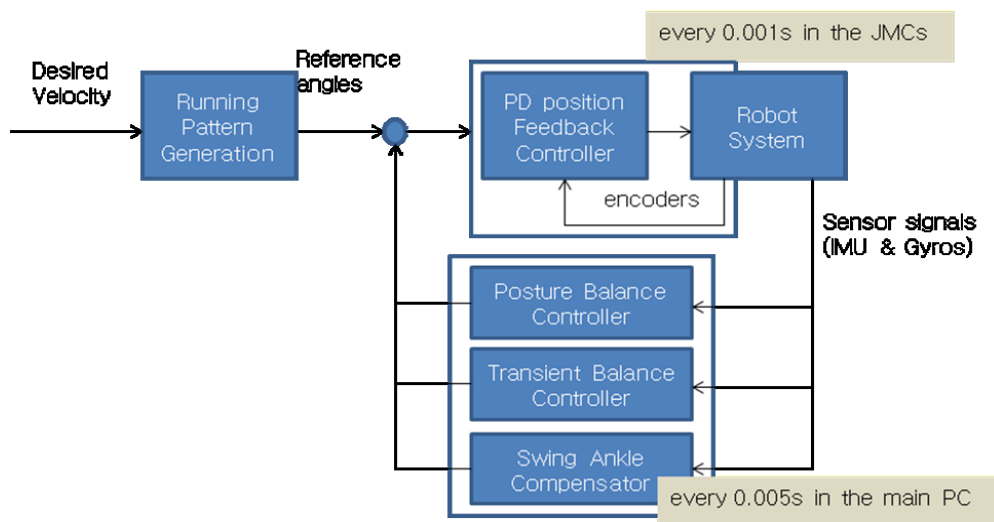

Figure 2. Structure of control system

The online controller of the HUBO2 used in this research is composed of two control loops, as shown in Fig. 2. The first control loop is concerned with the position control of the motor, and it works every 1 millisecond inside of the JMC. A general PD feedback controller is used here. The second control loop includes the online controller for running; this one works every 5 milliseconds, which is the same as the timer interrupt of the main computer. The main computer generates the position command for each joint motor by adding the reference angles of the offline running pattern

generator with the results of the online controllers. Then, the computer sends the motor command to the JMCs via CAN. These are the important roles of the main computer. The online controller for running is composed of three controllers, which are the posture balance controller in the sagittal plane, the transient balance controller in the frontal plane, and the swing ankle compensator in the sagittal plane. Since running is a larger and faster movement than walking, instability of the robot can easily be caused. So it is very important to maintain stability. In our algorithm, the balance is basically kept by the posture balance controller in the sagittal plane and the transient balance controller in the frontal plane. With the increase in velocity, the robot can fluctuate back and forth rather than left and right. At such times, the swing foot of the robot can touch the ground at an unexpected time and increase the instability. To prevent this phenomenon, the swing ankle compensator is added in the sagittal plane.

3.1. Posture Balance Controller in the Sagittal Plane

The humanoid robot has compliant effect due to a geometrical structure of the humanoid robot, reducer, the synthetic resins of the sole, compliant F/T sensor and harmonic drive gear. This compliant effect makes a vibration when the robot stands on the ground and the vibration causes instability. Therefore, a posture balance controller in the sagittal plane is proposed to reduce the vibration and keep the balance. This controller is applied only in the sagittal plane. The controller allows the robot to maintain its posture.

3.1.1. System Identification

To design the posture balance controller in the sagittal plane, the humanoid robot in the sagittal plane is simplified, as shown in the model in Fig. 3. m is the total mass of the robot, u is the position command of the motor, g is gravity, and L is the distance from the ankle joint to the COM(Center

of Mass). Also, the compliance of the robot is composed of a spring (K) and a damper (C). And, θ is the real angle of the robot against gravity, which is measured by the IMU sensor attached at the upper body.

The dynamic equation of the simple model is as given below.

$$mL^2\ddot{\theta} = -C\dot{\theta} - K(\theta - u) + mgL\sin\theta \tag{1}$$

Equation (1) is linearized as given below.

$$mL^2\ddot{\theta} + C\dot{\theta} + K\theta - mgL\theta = Ku \tag{2}$$

The transfer function between θ and u is as given below.

$$TF \equiv G(s) = \frac{\Theta(s)}{U(s)} = \frac{K}{mL^2 s^2 + Cs + (K - mgL)}$$

$$= \frac{\dfrac{K}{mL^2}}{s^2 + \dfrac{C}{mL^2}s + \dfrac{K - mgL}{mL^2}} = \frac{\dfrac{K}{mL^2}}{s^2 + 2\varsigma\omega_n s + \omega_n^2} \tag{3}$$

The unknown values of the transfer function are K and C. They are calculated through the analysis of the free vibration response of the robot. The vibration frequency (f_d) and the real number (σ) of pole of the free vibration response are easily estimated. With f_d and σ, the undamped natural frequency (ω_n) and the damping ratio (ς) are calculated as follows.

$$\sigma = \varsigma\omega_n$$

$$f_d = \frac{\omega_d}{2\pi}$$

$$\omega_d = \omega_n\sqrt{1-\varsigma^2} = \sqrt{\omega_n^2 - \sigma^2}$$

$$\therefore \omega_n = \sqrt{\omega_d^2 + \sigma^2} = \sqrt{(2\pi f_d)^2 + \sigma^2} \quad \text{and} \quad \varsigma = \frac{\sigma}{\omega_n} \tag{4}$$

Therefore, K and C are calculated as follows.

$$K = mL^2\omega_n^2 + mgL$$
$$= mL^2((2\pi f_d)^2 + \sigma^2) + mgL \tag{5}$$

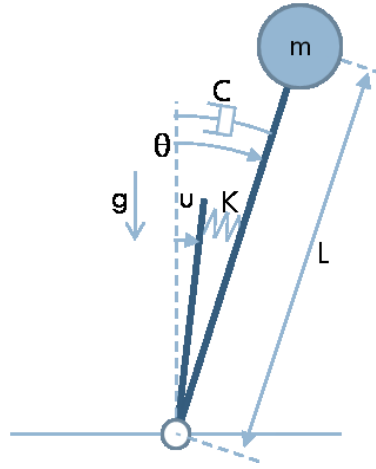$$C = 2\varsigma\omega_n mL^2 = 2\frac{\sigma}{\omega_n}\omega_n mL^2 = 2\sigma mL^2 \tag{6}$$

Figure 3. Simple model in the sagittal plane

Fig. 4 shows the free vibration response of HUBO2 in the sagittal plane. Therefore, f_d and σ were estimated as given below.

$$\sigma \approx 0.9$$

$$f_d \approx 1.17 Hz$$

With equation (4), ω_n and ς were calculated.

$$\omega_n \approx 7.4 \, rad/sec$$

$$\varsigma \approx 0.12$$

With equations (5) and (6), K and C were calculated.

$$K \approx 753 \, Nm/rad$$

$$C \approx 18 \, Nm/rad/sec$$

Therefore, the transfer function for a simple model of HUBO2 is as given below.

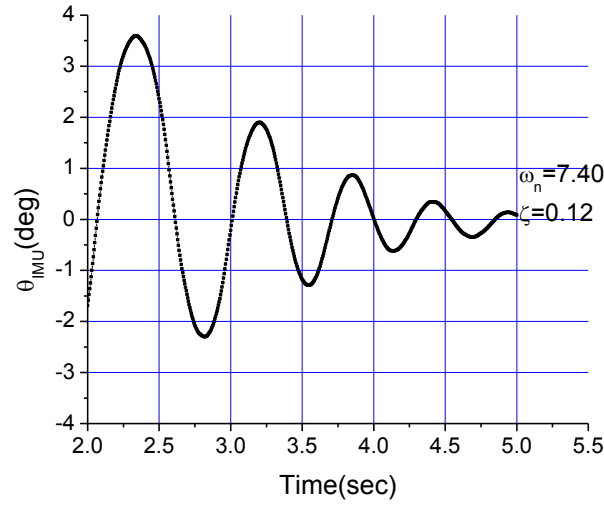$$TF \equiv G(s) \approx \frac{75.3}{s^2 + 1.8s + 54.9} \tag{7}$$

Figure 4. Free vibration response in the sagittal plane

3.1.2. Design of the Posture Balance Controller in the Sagittal Plane

The control law is as given below.

$$
\begin{aligned}
u_{AnklePitch} &= \theta^{Ref}_{AnklePitch} + \theta^{Control}_{AnklePitch} \\
&= \theta^{Ref}_{AnklePitch} + C_{Filter} K_P (\theta^{Ref}_{AnklePitch} - \theta^{IMU}_{AnklePitch})
\end{aligned}
\tag{8}
$$

$\theta^{Ref}_{AnklePitch}$ means the pre-scheduled ankle trajectory in the running pattern generation, $\theta^{Control}_{AnklePitch}$ means the control input created by the posture balance controller. The posture balance controller uses a P-controller. The structure of the posture balance controller in the sagittal plane is shown in Fig. 5.
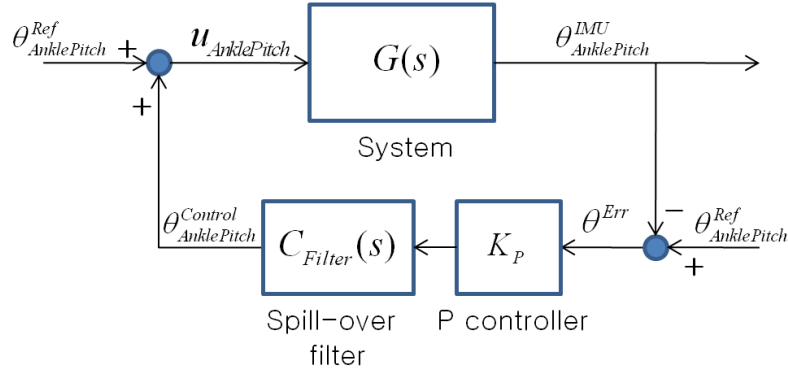
Figure 5. Block diagram of the posture balance controller in the sagittal plane

The transfer function of the simple model applied the posture balance controller is as follows.

$$U = R + C_{Filter}K_P E$$

$$E = R - \Theta$$

$$\Theta = GU = G(R + C_{Filter}K_P(R - \Theta))$$

$$(1 + C_{Filter}K_P G)\Theta = (G + C_{Filter}K_P G)R$$

$$\therefore \frac{\Theta(s)}{R(s)} = \frac{G + C_{Filter}K_P G}{1 + C_{Filter}K_P G} \tag{9}$$

U, R, E and Θ indicate the Laplace transforms of $u_{AnklePitch}$, $\theta^{Ref}_{AnklePitch}$, θ^{Err} and $\theta^{IMU}_{AnklePitch}$. G is the transfer function of the simple model and K_P is the gain of the posture balance controller. C_{Filter} is the transfer function of the spill-over filter. The spill-over filter prevents the unpredicted response caused by the difference between the real humanoid robot and the simple model. K_P is calculated by the root locus design method.

According to this procedure, the posture balance controller in the sagittal plane of HUBO2 is designed. The characteristic equation of the system applied controller is as given below.

$$1 + K_P C_{Filter}G(s) = 0 \tag{10}$$

Here,

$$C_{Filter}(s) = \frac{10}{s + 10} \tag{11}$$

$$G(s) = \frac{75.3}{s^2 + 1.8s + 54.9} \tag{12}$$

The root locus of the characteristic equation (10) is shown in Fig. 6 and 7. Fig. 6 shows the root locus when K_P is larger than zero (negative feedback), and Fig. 7 shows the root locus when K_P is smaller than zero (positive feedback). If K_P is set to a positive value, the system diverges. Therefore, K_P is set to a negative value.

K_P is set to -0.5 in this research. When K_P is -0.5, the damping ratio (ς) becomes 0.59. It is 4.9 times larger than the damping ratio when the posture balance controller is not applied. Since K_P is a negative value, the posture balance controller is the positive feedback controller.
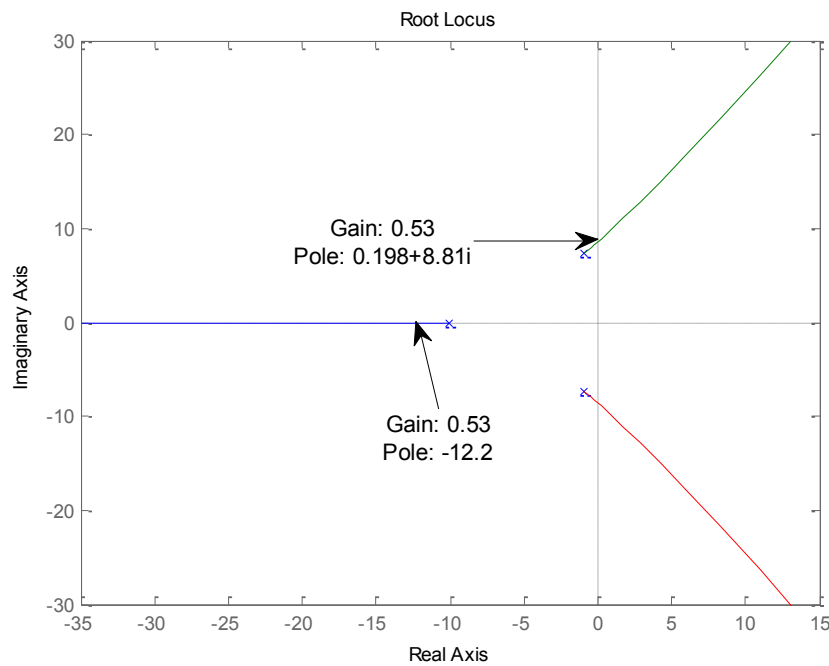

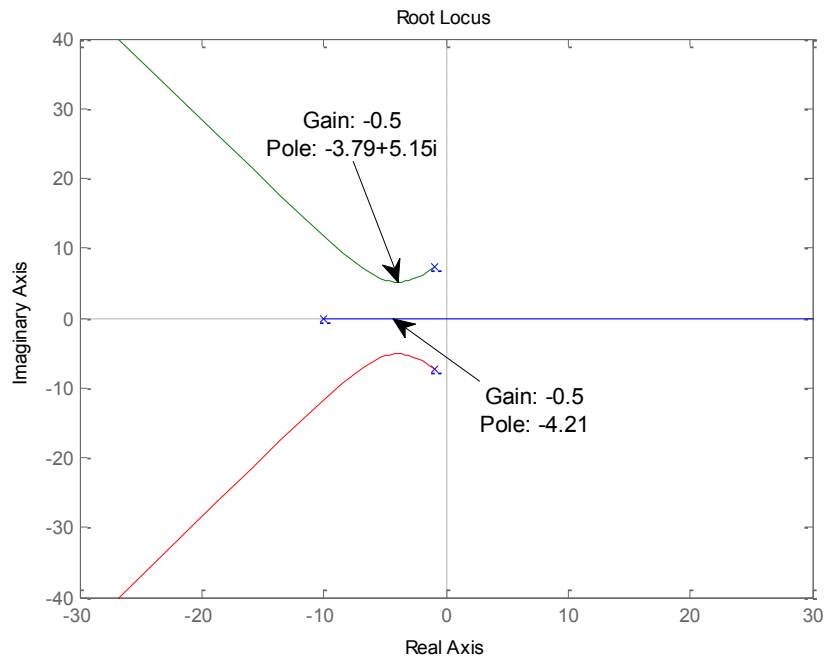**Figure 6.** Root locus of negative feedback

Figure 7. Root locus of positive feedback

3.2. Transient Balance Controller in the Frontal Plane

In the previous section, the IMU sensor attached at the upper body was used for the posture balance control. However, because the mechanical structure in the frontal plane is a cantilever beam structure, the upper body vibrates largely rather than the stance leg after landing. Therefore, the IMU sensor is not proper for balancing in the frontal plane. To solve this, gyros attached at the both thighs are used to make stability in the frontal plane.

A simple model of the humanoid robot in the frontal plane is shown in Fig. 8. When the robot stands on a single leg, it is assumed to be a single mass inverted pendulum, the same as the simple model in the sagittal plane. Rate gyros attached to both thigh parts measure the inclination rate of the stance leg. When the robot stands on its right leg, the rate gyro attached to the right thigh is used. When the robot stands on its left leg, the rate gyro attached to the left thigh is used. $\theta_{AnkleRoll}^{Ref}$ means the pre-scheduled ankle roll trajectory in the running pattern generation, $\dot{\theta}_{AnkleRoll}^{Gyro}$ is the angular velocity of the stance leg measured by the rate gyro, and $u_{AnkleRoll}$ indicates the control input created by the transient balance controller.

Fig. 9 shows the control structure of the transient balance controller in the frontal plane. The role of the transient balance controller is recovering the inclination rather than the running trajectory command with the ankle-roll joint in the frontal plane.

Similar to the system in a PD feedback controller, angle and angular velocity of the stance leg are used to calculate the control input. Since the rate gyro measures only angular velocity, the angle is estimated by the integration of the rate gyro. The real angle and the estimated angle are different because of the drift of the rate gyro signal. Therefore, the drift of the rate gyro is eliminated by the high pass filter and the integrator. Also, a spill-over filter is used to prevent unpredicted responses caused by differences between the real humanoid robot and the simple model.

The control law is as given below.

$$u_{AnkleRoll} = \theta_{AnkleRoll}^{Ref} + \theta_{AnkleRoll}^{Control}$$

$$= \theta_{AnkleRoll}^{Ref} + \frac{a_1}{s+a_1} \left(\frac{K_P}{s+a_2} + K_D \right) \left(\dot{\theta}_{AnkleRoll}^{Ref} - \dot{\theta}_{AnkleRoll}^{Gyro} \right) \quad (13)$$

The structure of the transient balance controller in Fig. 9 is somewhat similar to that of the posture balance controller in Fig. 5, but the physical action of the controller is different. When the humanoid robot runs forward, it moves in the same direction regardless of the stance foot in the sagittal plane. Thus, the performance in the steady state is significant. However, since the direction of the motion in the frontal plane is changed every step, the performance in the transient state is more significant to make a balance. Therefore, on the basis of the experimental experience, we use a negative feedback control in the transient balance controller. That is, the values of K_P and K_D applied to HUBO2 are positive. In the experiment, we decided that K_P is 0.3, K_D is 0.03, a_1 is 0.3, and a_2 is 0.6.
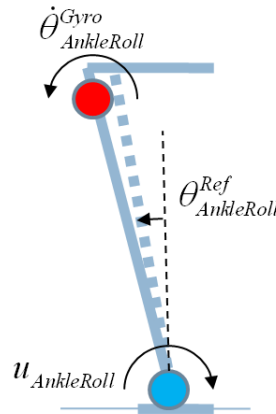

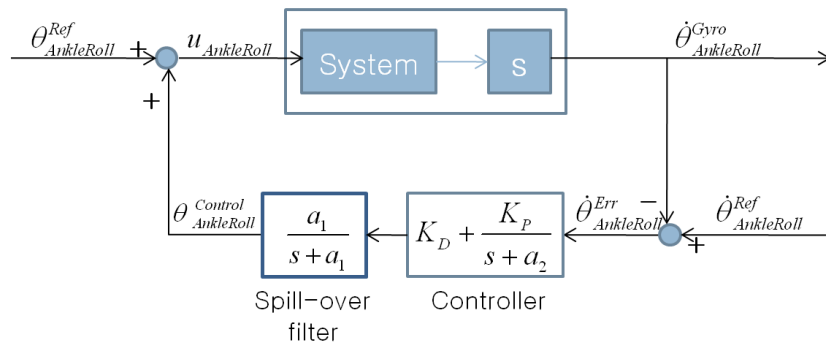**Figure 8.** Simple model in the frontal plane

Figure 9. Block diagram of transient balance control in the frontal plane

3.3. Swing Ankle Pitch Compensator in the Sagittal Plane

When the humanoid robot runs forward, it can be inclined forward or backward due to environmental factors. When it is inclined forward, the toe of the swing foot is able to touch the ground and this makes unstable running. Therefore, the toe of the swing foot is lifted up as shown in Fig. 10, according to the upper body's inclination. The inclination of the upper body is measured by the IMU sensor.

The control law is as given below.

$$
\begin{aligned}
u_{Swing} &= \theta_{Swing}^{Ref} + \theta_{Swing}^{Control} \\
&= \theta_{Swing}^{Ref} + \left(K_P + sK_D\right)\left(\theta_{Swing}^{Ref} - \theta_{Swing}^{IMU}\right)
\end{aligned} \quad (14)
$$

u_{Swing} is the input of the ankle pitch joint of the swing foot, θ_{Swing}^{Ref} is the desired trajectory of the ankle pitch joint of the swing foot, and θ_{Swing}^{IMU} is the estimated angle of the ankle pitch joint of the swing foot based on the IMU sensor.
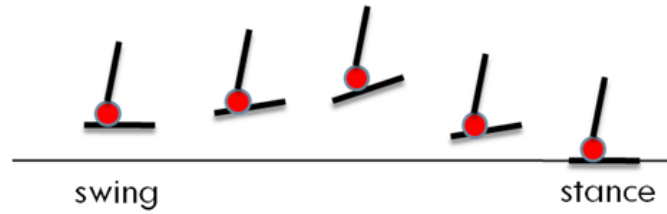

Figure 10. Motion of the swing foot

4. Experiments

The proposed controllers were applied to the humanoid robot HUBO2. Fig. 11 shows the experimental results according to the existence of the posture balance controller in the sagittal plane. At this time, the transient balance controller and the swing ankle pitch compensator are working. The solid line denotes the error between the desired angle and the real angle measured by the IMU sensor of the upper body when the robot runs forward with the posture balance controller. And, the dashed line denotes the angle error of the upper body without the posture balance controller. When the

controller is used, the error varies between -2 degrees and 2 degrees and the amplitude and period are regular, as shown in Fig. 11. That is, the running is stable with the posture balance controller. On the other hand, when the controller is not used, the error is larger than the error of the controlled system and the amplitude and period are irregular. To show the experimental results in detail, the phase portraits are plotted in Fig. 12. The left side of Fig. 12 is the phase portrait when the posture balance controller is activated and the right side of Fig. 12 is the phase portrait without activation of the controller. When the controller is used, the regular cycle is centered near the origin. On the other hand, when the controller is not used, the cycle is large and irregular. Therefore, we can see that the posture balance controller makes the robot run more stably.
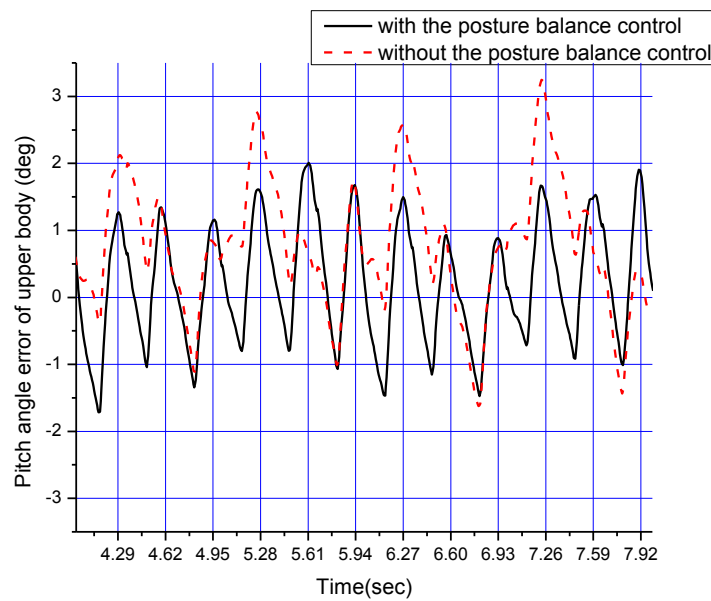

Figure 11. Experimental results of the posture balance control in the sagittal plane, speed: 2.52 km/h
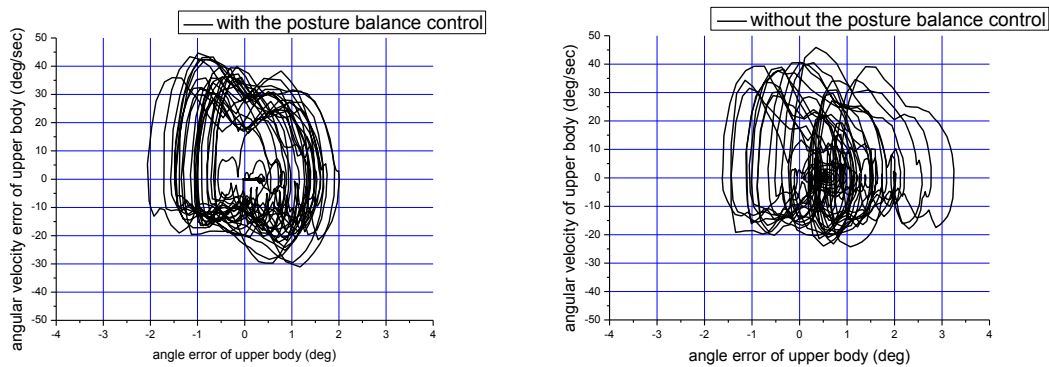
Figure 12. Phase portrait of the posture balance control in the sagittal plane, speed: 2.52 km/h

Also, Fig. 13 and 14 show the experimental results according to the existence of the transient balance controller in the frontal plane. The experiment was performed while the robot hopped in place, since the motion in the frontal plane is not closely related to the forward speed, unlike the motion in the sagittal plane. Even though the experiment only shows the case of hopping in place, this controller will still be effective when the robot runs at various speeds. During this experiment, the posture balance controller is always operating to reduce instability in the sagittal plane. In Fig. 13 and 14, the solid line is the error between the desired upper body angle and the measured upper body angle in the frontal plane, and the dashed line is the heavily low-pass filtered error, which means the center of oscillation of the error. When the controller is used (Fig. 13), the error is between -5 degrees and 6 degrees, and the amplitude and period of oscillation are regular. In addition, the center of the oscillating signal, the dashed line, is close to the x-axis, just like a straight line. That is, even though the robot vibrates in detail, the macro movement maintains a zero position. On the other hand, when the controller is not used (Fig. 14), the error is between -8 degrees and 6 degrees, and the amplitude and period of oscillation are more irregular. Also, the center of oscillation drifts. In Fig. 15, the phase portrait is also shown. The left figure shows the controlled signal and the right figure shows the uncontrolled signal. The controlled signal makes a regular cycle, whereas the uncontrolled signal shows an irregular and large shaken cycle. Therefore, the transient balance controller

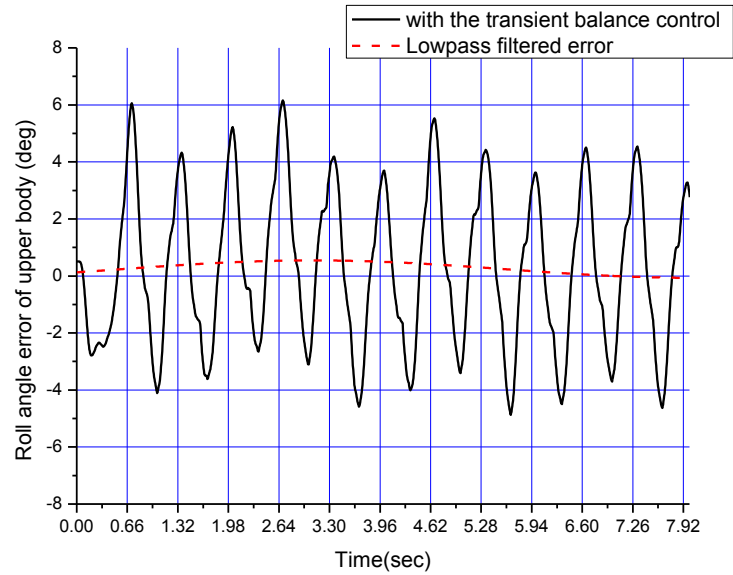makes the robot run more stably in the frontal plane.

Figure 13. Experimental results with the transient balance control in the frontal plane, speed: 2.52 km/h
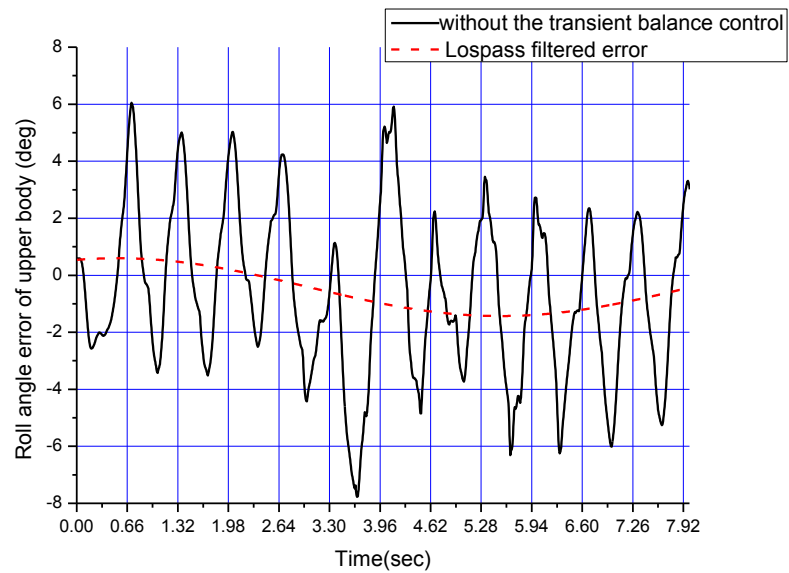

Figure 14. Experimental results without the transient balance control in the frontal plane, speed: 2.52 km/h
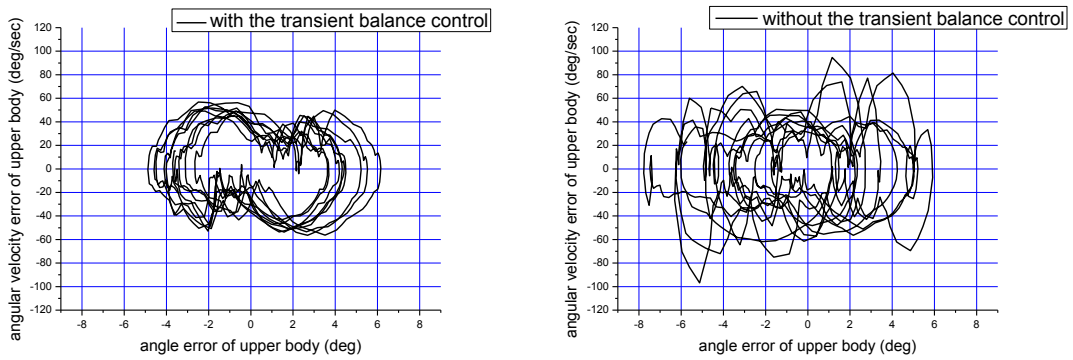
Figure 15. Phase portrait of the transient balance control in the frontal plane, speed: 2.52 km/h

Finally, a running experiment was performed to verify the performance of the proposed three online controllers. With the proposed controllers, stable running was successfully achieved. Fig. 16 shows a series of pictures in which HUBO2 ran. A video clip of this experiment can be seen on the website, http://hubolab.kaist.ac.kr.

Figure 16. Photo sequence of the running experiment of HUBO2

Table 2 shows the experimental results. HUBO2 can run at a maximum speed of 3.24km/h. The

running cycle is 0.33seconds and the step length is 0.30m. In addition, the flight time is 0.04sec and the flight length is 0.036m.

Table 2. Experimental Result

Maximum Running Speed	3.24km/h (0.9m/s)
Running Cycle	0.33sec/step
Maximum Running Step Length	0.30m/step
Flight Time	0.04sec/step
Maximum Flight Length	0.036m/step

5. Conclusion

In this paper, online controllers are proposed to achieve stable running in a humanoid robot. The controllers are composed of a posture balance controller in the sagittal plane, a transient balance controller in the frontal plane, and a swing ankle pitch compensator in the sagittal plane. Controller effectiveness was verified in a running experiment. In the experiment, HUBO2 ran stably at speeds from 0 to 3.24km/h. The contribution of the posture balance control and transient balance control on the stability was also analyzed by experiments.

In the future, the humanoid robot will be improved so that it can move faster and more stably. Also, a controller to maintain the stability of the robot according to large disturbances will be developed.

References

1. http://world.honda.com/ASIMO/
2. I. W. Park, J. Y. Kim, J. H. Lee, and J. H. Oh, Mechanical Design of Humanoid Robot Platform KHR-3 (KAIST Humanoid Robot -3: HUBO), in: *Proc. 5th IEEE-RAS Int. Conf. on Humanoid Robots*, Tsukuba, pp. 321-326 (2005).

3. K. Kaneko, F. Kanehiro, S. Kajita, H. Hirukawa, T. Kawasaki, M. Hirata, K. Akachi, and T. Isozumi, Humanoid Robot HRP-2, in: *Proc. Int. Conf. on Robotics & Automation*, New Orleans, LA, pp.1083-1090 (2004).

4. T. Takenaka, T. Matsumoto, and T. Yoshiike, Real Time Motion Generation and Control for Biped Robot – 2nd Report: Running Gait Pattern Generation -, in *Proc. of the 2009 IEEE/RAS International Conference on Intelligent Robots and Systems*, pp. 1092-1099 (2009).

5. T. Takenaka, T. Matsumoto, and T. Yoshiike, Real Time Motion Generation and Control for Biped Robot – 4nd Report: Integrated Balance Control -, in *Proc. of the 2009 IEEE/RAS International Conference on Intelligent Robots and Systems*, pp. 1601-1608 (2009).

6. R. Tajima, D. Honda, and K. Suga, Fast Running Experiments Involving a Humanoid Robot, in: *Proc. Int. Conf. on Robotics & Automation*, Kobe, pp. 1571–1576 (2009).

7. T. Ishida, Development of a Small Biped Entertainment Robot QRIO, in: *Proc. Int. Symp. on Micro-Nanomechatronics and Human Science*, Nagoya, pp. 23–28 (2004).

8. S. Kajita, T. Nagasaki, K. Kaneko, K. Yokoi and K. Tanie, A Running Controller of Humanoid Biped HRP-2LR, in: *Proc. Int. Conf. on Robotics & Automation*, Barcelona, pp. 618–624 (2005).

9. C. Chevallereau, E.R. Westervelt and J.W. Grizzle, Asymptotically Stable Running for a Five-link, Four-actuator, Planar Bipedal Robot, *Int. J. Robotics Res.* **24**, pp. 431–464 (2005).

10. Marc H. Raibert, *Legged Robots That Balance*, MIT Press, Cambridge, MA (1986).

11. B. K. Cho and J. H. Oh, Running Pattern Generation of Humanoid Biped with a Fixed Point and Its Realization, in: *Proc. 8th IEEE-RAS Int. Conf. on Humanoid Robots,* Daejeon, pp. 299–305 (2008).

12. S. Kajita, F. Kanehiro, K. Kaneko, K. Fujiwara, K. Harada, K. Yokoi and H. Hirukawa, Resolved Momentum Control: Humanoid Motion Planning Based on the Linear and Angular Momentum, in: *Proc. Int. Conf. on Intelligent Robots and Systems,* Sendai, pp. 1644–1650 (2003).

13. R. Tajima and K. Suga, Motion Having a Flight Phase: Experiments Involving a One-legged Robot, in: *Proc. Int. Conf. on Intelligent Robots and Systems*, Beijing, pp. 1726–1731 (2006).

14. M. Anthony Lewis, F. Tenore and R. Etienne-Cummings, CPG Design using Inhibitory Networks, in: *Proc. Int. Conf. on Robotics & Automation*, Barcelona, pp. 3682–3687 (2005).

15. K. Tadashi and H. Satomi, Control Method of Dynamic Biped Walking on Irregular Terrain using Neural Oscillators, in: *Proc. 7th Portuguese Conf. on Automatic Control, Lisbon,* pp. 247-258 (2006).

16. J. H. Kim and J. H. Oh, Realization of Dynamic Walking for the Humanoid Platform KHR-1, *Adv. Robotics*, **18**, pp. 749–768 (2004).

17. I. W. Park, J. Y. Kim, S. W. Park, and J. H. Oh, Development of Humanoid Robot Platform KHR-2(KAIST Humanoid Robot-2), in: *Proc. Int. Conf. on Humanoid Robots*, Los Angeles, CA, pp. 292–310 (2004).

18. J. Y. Kim, I. W. Park, J. H. Lee, M. S. Kim, B. K. Cho, and J. H. Oh, System Design and Dynamic

Walking of Humanoid Robot KHR-2, in: *Proc. Int. Conf. on Robotics & Automation*, Barcelona, pp. 1431–1436 (2005).

19. S. Kajita, K. Kaneko, M. Morisawa, S. Nakaoka and H. Hirukawa, ZMP-based Biped Running Enhanced by Toe Springs, in: *Proc. Int. Conf. on Robotics & Automation*, Roma, pp. 3963–3969 (2007).

Baek-Kyu Cho was born in Hong-Sung, South Korea, in 1980. He received the BS, MS, and PhD degrees in Mechanical Engineering from Korea Advanced Institute of Science and Technology (KAIST) in 2002, 2004, and 2009 respectively. In 2009, he was a Post-doctoral Researcher in KAIST. He is now with the Department of Brain Robot Interface (BRI), the Computational Neuroscience Laboratories (CNS), Advanced Telecommunications Research Institute International (ATR), Kyoto 619-0288, Japan, and also with the National Institute of Information and Communications Technology (NiCT), Kyoto 619-0288, Japan. His research interests include design and control of biped humanoid robot, walking and running pattern generations, and development of devices using micro processors.

Jung-Hoon Kim received the BS degree in Mechanical Design and Production Engineering from Yonsei University, and the MS and PhD degrees in Mechanical Engineering from KAIST in 1997, 1999 and 2004, respectively. From 2004 to 2005, he was a Post-doctoral Researcher in the University of California, Berkeley. From 2005 to 2006, he was a Senior Engineer at Mechatronics Center in Samsung Electronics. He is currently an Assistant Professor in the Department of Civil and Environmental Engineering, Yonsei University, Seoul, Korea. His research interests include design and control of biped humanoid robots, wearable exoskeleton robots, robotics in construction and infrastructure maintenance engineering. He is a member of the KSPE, ICROS, KSCE, and KICEM.

Jun-Ho Oh was born in Seoul, South Korea, in 1954. He received the BS and MS degrees in Mechanical Engineering from Yonsei University, Seoul, South Korea, and the PhD degree in Mechanical Engineering from the University of California, Berkeley, in 1977, 1979 and 1985, respectively. He was a Researcher with the Korea Atomic Energy Research Institute, from 1979 to 1981. Since 1985, he has been with the Department of Mechanical Engineering, KAIST, where he is currently a professor. He was a Visiting Research Scientist at the University of Texas, Austin, from 1996 to 1997. His research interests include humanoid robots, adaptive control, intelligent control, nonlinear control, biomechanics, sensors, actuators and applications of micro processors. He is a member of the IEEE, KSME, KSPE and ICASE.